Multiple attractors in grazing-sliding bifurcations in Filippov type flows

Paul Glendinning

School of Mathematics, The University of Manchester, Oxford Road, Manchester M13 9PL, U.K., Email: p.a.glendinning@manchester.ac.uk

Piotr Kowalczyk

School of Computing, Mathematics and Digital Technology, John Dalton Building, Manchester Metropolitan University, Chester Street, Manchester, M1 5GD, U.K., Email: p.kowalczyk@mmu.ac.uk

Arne B Nordmark

Department of Mechanics, KTH, 100 44 Stockholm, Sweden, Email: nordmark@mech.kth.se

Abstract

We describe two examples of three-dimensional Filippov type flows in which multiple attractors are created by grazing-sliding bifurcations. To the best of our knowledge these are the first examples to show multistability in the literature. In both examples we identify the coefficients of the normal form map describing the bifurcation, and use this to find parameters with the desired behaviour. In the first example this can be done analytically whilst the second is a classic dry friction model and the identification is numerical. This explicit correspondence between the flows and a truncated normal form map reveals an important feature of the sensitivity of the predicted dynamics normal form map: the scale of the variation of the bifurcation parameter past the grazing-sliding has to be very carefully chosen. Although no detailed analysis is given we believe that this may indicate a much greater sensitivity to parameters than experience with smooth flows might suggest. We conjecture that the grazing-sliding bifurcations leading to multistability remained unreported in the literature due to this sensitivity to parameter variations.

Keywords: grazing-sliding, multiple attractors, Filippov flows, explicit

example
2000 MSC: 05.45.Ac, 05.45 -a, 02.30.Oz

---

1. Introduction

The dynamics of systems with both continuous and discrete evolution has been the subject of many recent studies, see for instance [1, 4, 5, 8, 14]. This interest is motivated by the use of digital devices (microprocessors) which communicate with sensors that operate in continuous time in many industries, e.g. car industry, telecommunications or aerospace. Also, on the macroscopic level, there are many physical processes which can be modelled using a combination of continuous and discrete dynamics. Examples include genetic regulatory networks [6] which have recently been modelled using switched vector fields, power electronic converters [2, 3], mechanical systems friction, [13] or modern control systems [9].

Such systems have been shown to undergo topological transitions (bifurcations) which are triggered by a combination of both continuous and discrete dynamics. In particular, systems characterized by the presence of manifolds in phase space where continuous time evolution undergoes a sudden jump, either in state variables or its derivatives, have been shown to exhibit so called discontinuity induced bifurcations (DIBs for short). The manifolds across which switching takes place are called switching manifolds or discontinuity sets. A DIB can occur if a limit cycle has a tangential (or grazing) intersection with a discontinuity set. It has been shown that such an instance may cause a sudden onset of chaotic dynamics [7]. Another intriguing scenario, observed only in systems with discontinuity manifolds, is the possibility of the creation of multiple attractors triggered by a DIB [1, 10]. However, so far, such a scenario has been reported to occur only in piecewise smooth maps. In this paper we present an example of a Filippov type flow, that is a flow generated by the vector field which is discontinuous across the switching surface, where grazing-sliding bifurcation leads to the onset of multiple attractors. We believe that the multiple attractors found in our model example may occur in many systems of relevance to applications, and perhaps they can be utilised in developing control strategies; depending on the application certain type of an attractor may have a more desirable characteristics than another one, and by appropriate choice of system parameters we may force our system on the desired attractor. In particular, in Sec. 6 we present a

dry-friction oscillator model where grazing-sliding bifurcation leads to multistability of period-two and period-three limit cycles with a segment of sliding. This is the first instance of reporting this type of grazing-sliding bifurcation in dry-friction oscillator models.

Our analysis begins with the normal form of the grazing-sliding bifurcation, where parameter values have at which different forms of coexistence have been identified [11]. Ignoring higher order corrections these maps are piecewise linear, and so there is no natural scale for the bifurcation parameter μ. However, the coefficients of the linear map are related to the Floquet multipliers of the grazing orbit and the first example is a toy model constructed so that this correspondence can be written down analytically. In the second (dry friction) example, the correspondence with the coefficients of the truncated normal form is calculated numerically. Thus in both cases we can identify the truncated normal form and hence we know the dynamics predicted by the normal form. Coefficients in the normal fom are chosen so that three qualitatively different bifurcations occur: (a) the creation of period-two and period-three stable orbits with one sliding segment, (b) a chaotic attractor coexisting with stable period-three orbit characterized by a segment of sliding motion, and (c) the coexistence of a period-three sliding orbit with two sliding segments and a limit cycle with no sliding segments. Thus, *in principle*, if parameters in the flows are chosen so that the coefficients of the truncated normal form are those selected, we know the dynamics immediately after bifurcation.

The numerical simulations presented here confirm the connection between the dynamics of the truncated normal form and the flows, but only for very small values of the bifurcation parameter. This sensitivity seems to be a common observation in numerical simulations; for example, this may be due to complicated configurations of bifurcations as in [16], where a similar analysis of flows via the truncated normal form is made. In that case multistability is seen in a smoothed version of the flow, though it is not predicted by the truncated normal form. However, we are not aware that this issue has ever been stated explicitly or explored. We believe this is potentially important and should be followed up (though we do not attempt this here). In the toy model one of the attractors (the period three orbit) is very sensitive to parameter variation and is soon lost, whilst in the dry friction model the same orbit undergoes a switching-sliding bifurcation [7], i.e. a new bifurcation due to global features of the flow not modelled by the normal form, soon after bifurcation.

The remainder of the paper is arranged as follows. In Sec. 2 the methodology used to construct the explicit toy example is described. In Sec. 3 the derivation of the linearized return map (truncated normal form) about the grazing-sliding bifurcation is derived. Parameters can be chosen such that the grazing orbit has complex Floquet multipliers. The method of determining the sliding vector field to obtain any truncated normal form is described in Sec. 4, and Sec. 5 is then devoted to presenting different cases of multistability described via maps in [11]. In Sec. 6 the coexistence of two stable periodic orbits is shown using the same techniques but for a standard dry friction model. Finally, in the conclusion, Sec. 7, we suggest one reason why greater sensitivity to the parameter might be more likely in these bifurcations.

2. A Model System

The starting point for the construction of a three-dimensional Filippov system with grazing and sliding for which all the relevant features (return map, switching surface, the coefficient of the sliding vector field) can be calculated explicitly, is a simple underlying flow with a periodic orbit. This flow needs to be chosen so that the (linearized) return map about the periodic orbit is easy to calculate analytically with sufficient freedom to be able to match any required linearization.

There are, no doubt, many ways to achieve this. We have chosen to start with a two-dimensional flow such that one axis (the $z-$axis) is invariant and restrict to the positive half-plane in the other variable (r). By arranging for the existence of a stable stationary point in $r > 0$ the simple expedient of rotating the entire half-plane by introducing a polar angle θ with $\dot{\theta} > 0$ produces a flow on $\mathbb{R}^3$ with a stable periodic orbit having fixed r and z coordinates.

The first step towards defining the motion in the $(r, z)-$ plane is to consider the system

$$\begin{aligned} \dot{r} &= -4kr + 2rz \\ \dot{z} &= 4\alpha^2 - r^2 - z^2. \end{aligned} \tag{1}$$

Stationary points of this equation have $r = 0$ or $z = 2k$ (from the $\dot{r}$ equation) and then if $r = 0$, $z = \pm 2\alpha$; whilst if $z = 2k$ then $r = 2\sqrt{\alpha^2 - k^2}$ provided $\alpha > k$. Fixed points in $r > 0$ correspond to periodic orbits of the full three-dimensional system, whilst fixed points with $r = 0$ are also fixed points of

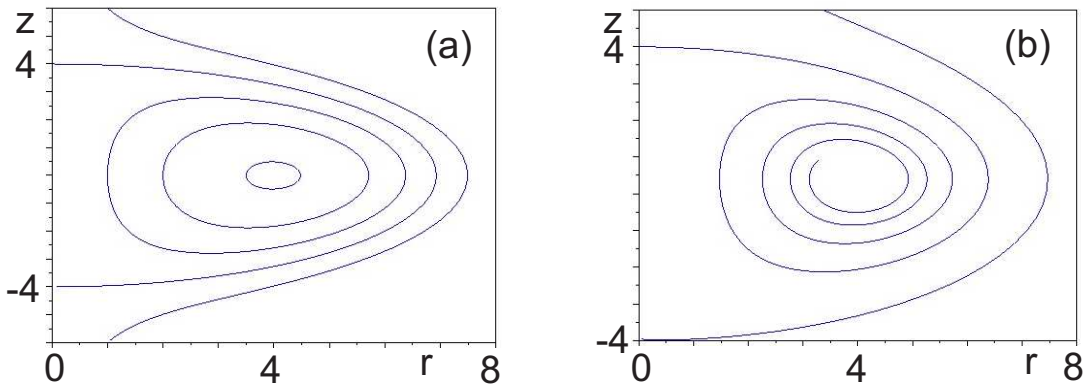

Figure 1: Solutions of the two dimensional flow: (a) $\alpha = 2$, $k = 0$; (b) $\alpha = 2$, $k = 0.2$.

the full system. If $k = 0$ (1) is Hamiltonian, with Hamiltonian h defined by

$$h(z, r) = 4\alpha^2 r - rz^2 - \frac{1}{3}r^3$$

so $\dot{r} = -\frac{\partial h}{\partial z}$ and $\dot{z} = \frac{\partial h}{\partial r}$. If $k \neq 0$ then the stationary point in $r > 0$ exists if $\alpha^2 > k^2$ and it is stable if $k > 0$ and unstable if $k < 0$,. It is a focus if $5k^2 < 4\alpha^2$ and a node if $5k^2 > 4\alpha^2 > 4k^2$. Sample phase portraits are shown in Figure 1.

Introducing an angle θ with $\dot{\theta} = \omega$, gives a flow in $\mathbb{R}^3$ which is given in cylindrical polar coordinates (r, θ, z) by

$$\begin{aligned} \dot{r} &= -4kr + 2rz \\ \dot{\theta} &= \omega \\ \dot{z} &= 4\alpha^2 - r^2 - z^2 \end{aligned} \tag{2}$$

or, in standard Cartesian coordinates,

$$\begin{aligned} \dot{x} &= -4kx - \omega y + 2xz \\ \dot{y} &= \omega x - 4ky + 2yz \\ \dot{z} &= 4\alpha^2 - x^2 - y^2 - z^2 \end{aligned} \tag{3}$$

This system has a periodic orbit if $\alpha^2 > k^2$ with $r = 2\sqrt{\alpha^2 - k^2}$, $z = 2k$ and $0 \leq \theta < 2\pi$. This is the stationary point of the two-dimensional system rotated about the $z-$axis. In the next section we analyze this periodic orbit, deriving an explicit formula for the linear part return map near the periodic orbit on the plane $y = 0$. We can then create a Filippov system by defining a flow on a half-space, e.g. $x < 2\sqrt{\alpha^2 - k^2} + \mu$.

3. The linearized return map

Suppose that $5k^2 < 4\alpha^2$, so the periodic orbit of the full system exists and has period $\frac{2\pi}{\omega}$. Consider a small perturbation starting on the surface $\theta = 0$ at $t = 0$, and write

$$z = 2k + u, \quad r = 2\sqrt{\alpha^2 - k^2} + v, \quad |u|, |v| \ll 1.$$

Substituting into (1) and ignoring higher order terms gives the linearized system

$$\begin{aligned} \dot{u} &= -4ku - 4\sqrt{\alpha^2 - k^2}v \\ \dot{v} &= 4\sqrt{\alpha^2 - k^2}u \end{aligned} \tag{4}$$

or

$$\ddot{v} + 4k\dot{v} + 16(\alpha^2 - k^2)v = 0 \tag{5}$$

with characteristic equation $s^2 + 4ks + 16(\alpha^2 - k^2) = 0$ having roots $-2k \pm 2\sqrt{5k^2 - 4\alpha^2}$. Let $\Omega^2 = 4(4\alpha^2 - 5k^2)$, $\Omega > 0$, so the roots are $-2k \pm i\Omega$ and the solution of (5) is

$$v = e^{-2kt}\left(A\cos\Omega t + B\sin\Omega t\right) \tag{6}$$

and the second equation of (4) implies

$$u = \frac{e^{-2kt}}{4\sqrt{\alpha^2 - k^2}}\left((-2kA + B\Omega)\cos\Omega t + (-2kB - A\Omega)\sin\Omega t\right). \tag{7}$$

Now suppose that at $t = 0$ $(v, u) = (v_0, u_0)$, so in terms of the full three-dimensional system u_0 is the perturbation from the periodic orbit in the $z-$coordinate, and v the perturbation in the $x-$coordinate on the plane $y = 0$, then

$$A = v_0, \quad B = \frac{1}{\Omega}(4\sqrt{\alpha^2 - k^2}u_0 + 2kv_0)$$

and after a time of $\frac{2\pi}{\omega}$ the solutions return to the plane $y = 0$ with perturbations (v_1, u_1) where

$$\begin{pmatrix} v_1 \\ u_1 \end{pmatrix} = \begin{pmatrix} a_{11} & a_{12} \\ a_{21} & a_{22} \end{pmatrix} \begin{pmatrix} v_0 \\ u_0 \end{pmatrix} \tag{8}$$

with, setting $E = \exp(-4\pi k/\omega)$,

$$\begin{aligned} a_{11} &= E(\cos\tfrac{2\pi\Omega}{\omega} + \tfrac{2k}{\Omega}\sin\tfrac{2\pi\Omega}{\omega}) \\ a_{12} &= \tfrac{4\sqrt{\alpha^2-k^2}E}{\Omega}\sin\tfrac{2\pi\Omega}{\omega} \\ a_{21} &= \tfrac{E}{4\sqrt{\alpha^2-k^2}}(-\Omega - \tfrac{4k^2}{\Omega})\sin\tfrac{2\pi\Omega}{\omega} \\ a_{22} &= E(\cos\tfrac{2\pi\Omega}{\omega} - \tfrac{2k}{\Omega}\sin\tfrac{2\pi\Omega}{\omega}). \end{aligned} \tag{9}$$

Note that consideration of the divergence of the vector field in (1) shows that the determinant of the matrix (9) is E^2, which can be verified directly from (9), so if we refer to this matrix as R then

$$\det\ R = E^2 = \exp(-8\pi k/\omega), \quad \text{Tr}\ R = 2E\cos\frac{2\pi\Omega}{\omega} \tag{10}$$

and so, with $\omega = 1$, we can choose det R via k and then Tr R using α.

It is equally possible to treat the case of real eigenvalues, but the complex eigenvalue case is the one discussed in [11], so we stop the analysis here.

4. Constructing the sliding motion

In [11] the parameters for multistability are specified in coordinates in which the linear map near the periodic orbit takes the form

$$\begin{pmatrix} T & 1 \\ -D & 0 \end{pmatrix} \tag{11}$$

and since we are working in a different set of coordinates we will need to take care that the coefficients are those corresponding to the correct choice of coordinates. For simplicity we will place the sliding bifurcation parameter μ in the switching surface H rather than in the differential equation and consider

$$\dot{\mathbf{x}}(t) = \begin{cases} F_1(\mathbf{x}(t)) & if \quad H(\mathbf{x}(t),\mu) > 0 \\ F_2(\mathbf{x}(t)) & if \quad H(\mathbf{x}(t),\mu) < 0, \end{cases} \tag{12}$$

where F_1, F_2 are sufficiently smooth vector functions, F_1, $F_2 : \mathbb{R}^3 \mapsto \mathbb{R}^3$ and $H(\mathbf{x}(t),\mu) : \mathbb{R}^3 \times \mathbb{R} \mapsto \mathbb{R}^3$ is some smooth scalar function depending on system states $\mathbf{x} \in \mathbb{R}^3$, and parameters $\mu \in \mathbb{R}$; $t \in \mathbb{R}$ is the time variable.

We will work with

$$H(\mathbf{x},\mu) = 2\sqrt{\alpha^2 - k^2} + \mu - x \tag{13}$$

and F_1 defined by (1) with the fixed parameters chosen below to satisfy the criteria of [11] for multistability. These choices imply that the periodic orbit analyzed in the previous section lies entirely in the region $H(\mathbf{x},\mu) > 0$ (where the Filippov flow is defined by F_1) provided $\mu > 0$. If $\mu = 0$ then the periodic orbit grazes H at the point $(2\sqrt{\alpha^2 - k^2}, 0, 2k)$, whilst if $\mu < 0$ then the periodic orbit intersects the switching surface transversally at two points

(for small μ) and the flow near the periodic orbit will depend on the choice of F_2 in (12). The linear approximation of the PDM (see [8] for a detailed derivation) can be written as

$$PDM(X,Z) = \begin{cases} \mathbf{X} & \text{for} \quad X > 0 \\ \begin{pmatrix} 0 & 0 \\ \hat{C} & 1 \end{pmatrix} \begin{pmatrix} X \\ Z \end{pmatrix} & \text{for} \quad X \leq 0 \end{cases} \tag{14}$$

in terms of shifted local coordinates $\mathbf{X} = (X, Z)$ on $\{y = 0\}$. The constant $\hat{C}$ is a function of the vector field $F_2 = (F_2^x,\, F_2^y,\, F_2^z)^T$ and the Jacobian matrix f_{ij} of F_1 evaluated at the grazing point:

$$\hat{C} = -\frac{F_2^z}{F_2^x} + \left(\frac{f_{11}}{f_{12}} + f_{12} \frac{F_2^z}{F_2^x} \right) F_1^z. \tag{15}$$

The choice of PDM used in [11] to derive conditions for multistability is in coordinates in which the linear map takes the form given by (11) with the coefficient $\hat{C}$ replaced by C, with the relation between the coefficients given by

$$C = a_{22} + \hat{C} a_{12}. \tag{16}$$

We end this section with a brief explanation of these formulae. Following [8] we can write the two-dimensional PDM, in the case of a three-dimensional Filippov type flow and using (X, Z) coordinates, as

$$PDM(X, Z, q; \mu) = \begin{pmatrix} X \\ Z \end{pmatrix} + \beta(X, Z, q; \mu) q^2, \tag{17}$$

where

$$q^2 + H(X, Z; \mu) = 0$$

with q being an independent variable that measures the penetration of trajectories below the switching surface for orbits sufficiently close to the grazing orbit. The coordinates (X, Z) are chosen such that the grazing incidence takes place at $(X, Z, q; \mu) = (0, 0, 0; 0)$. The linearization of (17) at grazing gives

$$PDM_L(X, Z, q; \mu) = \begin{pmatrix} X \\ Z \end{pmatrix} - \beta(0,0,0;0) \langle H_x, [X, Z] \rangle - \beta(0,0,0;0) H_\mu \mu, \tag{18}$$

where

$$\beta(0,0,0\,0) = \frac{1}{\langle H_x, (F_2 - F_1)\rangle} F_2 + \frac{\langle (H_x F_1)_x, F_2\rangle}{\langle (H_x F_1)_x, F_1\rangle} F_1$$

with the right-hand side evaluated at the grazing point $(0,0,0;0)$, and $\langle , \rangle$ denoting the standard dot product. At grazing the X-component of the vector field F_1 is zero. Using the definition of the switching function and ignoring the parameter dependence we arrive at the map (14) given above.

5. The example and multistability

Qualitatively different types of multistability which can be observed in the particular case of a grazing-sliding bifurcation scenario are dependent on the trace T, determinant D of the linear map (10), and the coefficient C given in (16), which is also a non-trivial Floquet multiplier of the grazing limit cycle with a zero-length sliding segment. We note that the grazing limit cycle can be viewed as a limit cycle with no sliding segments or as having a zero-length sliding segment (see [12] for further details).

5.1. Case I: Two stable orbits

As we proved in [11] multistability corresponding to the co-existence of period-two and period-three orbits with a sliding segment will be observed in a grazing-sliding bifurcation provided that $1 > T > 0$, $D > T^2$, $-C > 1$ and $T < \dfrac{-C-1}{C^2+C+1}$. These conditions are sufficient. The necessary conditions are not known.

We now take a specific example of multistability from [11]: $T = 0.05$, $D = 0.31$ and $C = -3$. Using (10) we require

$$0.31 = E^2 = \exp(-8\pi k/\omega), \quad 0.005 = 2E\cos\left(\frac{2\pi\Omega}{\omega}\right).$$

By setting $\omega = 1$ we find $\alpha = 0.08$ and $k = 0.0466$. In our case $F_1^z = 0$ and since $F_2^x < 0$, if we let $F_2^x = -1$, we then have $F_2^z = -4.7192$. A stable period-three orbit with a sliding segment is depicted in Fig. 2 and a stable period-two orbit in Fig. 3.

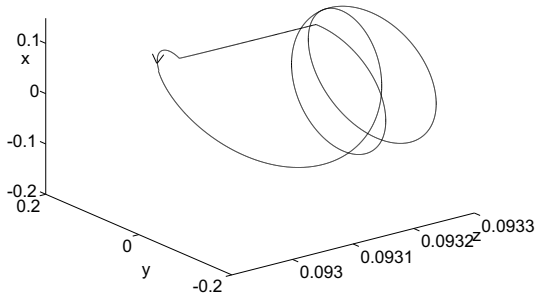

Figure 2: Stable period-3 orbit with sliding for $\omega = 1$, $k = 0.0466$ and $\alpha = 0.08$, with the initial condition $[x,\, y,\, z]^T = [0.036291,\, 0.124810,\, 0.093028]^T$ and $\mu = -0.000005$

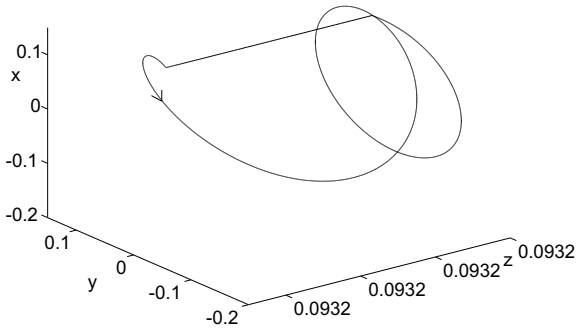

Figure 3: Stable period-2 orbit with sliding for $\omega = 1$, $k = 0.0466$ and $\alpha = 0.08$, with the initial condition $[x,\, y,\, z]^T = [-0.028117,\, -0.126974,\, 0.093209]^T$ and $\mu = -0.000005$

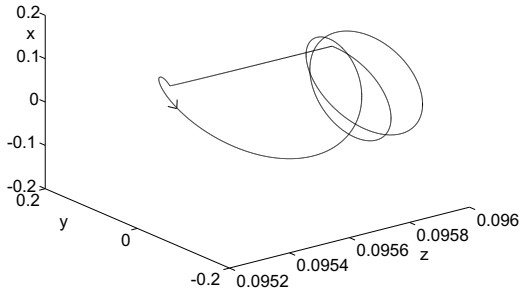

Figure 4: Stable period-3 orbit with sliding for $\omega = 1$, $k = 0.04790$, $\alpha = 0.07297$ and $\mu = -0.00005$, with the initial condition $[x,\, y,\, z]^T = [0.0259013,\, 0.1067204,\, 0.0959262]^T$

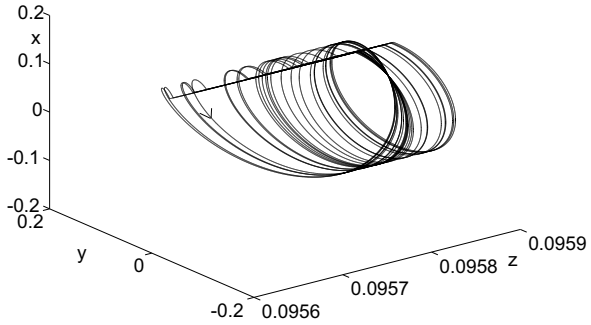

Figure 5: Chaotic attractor for $\omega = 1$, $k = 0.04790$, $\alpha = 0.07297$ and $\mu = -0.00005$. The initial condition $[x,\, y,\, z]^T = [-0.085976,\, -0.068551,\, 0.095775]^T$

5.2. Case II: A stable orbit and a chaotic attractor

The second case of multistability reported in [11] is the case of a chaotic attractor coexisting with a stable periodic orbit with sliding. This scenario was found for $T = 0.35$, $D = 0.3$ and $C = -3$. Fixing $\omega = 1$ gives $k = 0.04790$, $\alpha = 0.07297$ and $F_2^Z = -5.0727$ (for $F_2^x = -1$). A stable period-three orbit is depicted in Fig. 4 and a chaotic attractor in Fig. 5.

5.3. Case III: A stable orbit with sliding and a stable non-sliding orbit

The last case of multistability reported in [11] is that of a stable period-3 orbit coexisting with a stable non-sliding orbit. Representative parameter values at which these attractors where reported to exist are $T = -0.1$, $D = 0.7$, $C = -1.8$ with $\mu > 0$. Fixing $\omega = 1$ gives $k = 0.01419$, $\alpha = 0.06679$,

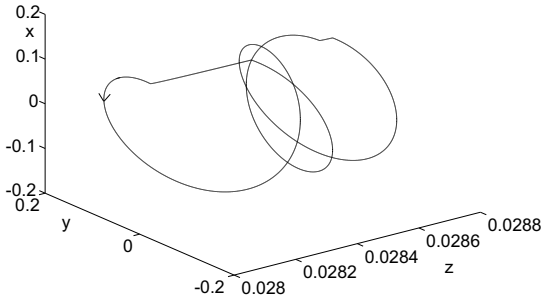

Figure 6: A stable period-3 orbit with two sliding segments for $\omega = 1$, $k = 0.01419$, $\alpha = 0.06679$ and $\mu = 5 \times 10^{-6}$. For the simulations the initial condition $[x,\, y,\, z]^T = [2\sqrt{\alpha^2 - k^2} + \mu + 10^{-4}, 10^{-5}, 2k]^T$ was used (we disregard the transient).

and $F_2^Z = -1.97425287$ with $F_1^X = -1$. A period-three stable orbit detected for $\mu = 5 \times 10^{-6}$ is depicted in Fig. 6. A simple stable non-sliding periodic orbit (not shown) can also be found using the initial conditions $[x,\, y,\, z]^T = [0.129880,\, 0.013031,\, 0.028383]^T$.

6. Dry-friction oscillator model

We now consider a model of a dry-friction oscillator which consists of a mass m resting on a belt moving with a constant velocity. The mass is attached to a rigid wall through a damper and a nonlinear spring which is characterized by the cubic stiffness law (a Duffing oscillator model). The friction force between the moving belt and the mass resting on it is modelled by means of a discontinuous friction characteristic given by the Coulomb friction law:

$$F_{friction} = F_s \mathrm{sgn}(v_{\mathrm{rel}}), \tag{19}$$

where v_{rel} refers to the difference between the velocity of the driving belt and moving mass. The system equation is then given by

$$m\ddot{q} + c\dot{q} + \alpha_1 q + \alpha_2 q^3 = F_{friction} + A\cos(\omega t). \tag{20}$$

We will scale the time and position so that the frequency of the harmonic forcing and the amplitude of the friction force will be both set to 1. Introducing the non-dimensional time $\tau = \omega t$ and position $x = q\frac{m\omega^2}{F_s}$, we can

now rewrite (20) as

$$F_s\ddot{x} + \frac{F_s c}{m\omega}\dot{x} + \frac{\alpha_1 F_s}{m\omega^2}x + \frac{\alpha_2 F_s^3}{m^3\omega^6}x^3 = F_s \mathrm{sgn}(v_0 - \dot{x}) + A\cos(\tau). \tag{21}$$

Since $F_s > 0$, we have

$$\ddot{x} + \frac{c}{m\omega}\dot{x} + \frac{\alpha_1}{m\omega^2}x + \frac{\alpha_2 F_s^2}{m^3\omega^6}x^3 = \mathrm{sgn}(v_0 - \dot{x}) + \frac{A}{F_s}\cos(\tau). \tag{22}$$

Using non-dimensional parameters $p_1 = c/m\omega$, $p_2 = \alpha_1/m\omega^2$, $p_3 = \alpha_2 F_s^2/m^3\omega^6$ and $p_4 = A/F_s$, we can express (22) as

$$\ddot{x} + p_1\dot{x} + p_2 x + p_3 x^3 = \mathrm{sgn}(v_0 - \dot{x}) + p_4\cos(\tau), \tag{23}$$

where v_0 is the non-dimensionalized velocity of the moving belt.

We detected a grazing-sliding bifurcation leading to the onset of period-two and period-three stable orbits for $p_1 = 0.1864$, $p_2 = -5.862812$, $p_3 = 0.092913$, $p_4 = 3.333$ and $v_0^* = 14.770518$ where the grazing periodic point on the limit cycle is given by $[x, \dot{x}, \tau] = [7.9147, 14.7705, 1.1317]$. Decreasing v_0 to $v_0 = 14.769$ will lead to the creation of stable attractors of period-two and three (see Fig. 7), but if $v_0 = 14.765$ the period three orbit has changed – it has an extra segment in $\dot{x} > v_0$, i.e. it has undergone a switching -sliding bifurcation not present in the truncated normal form analysis.

We can easily verify conditions from Sec. 5 for the onset of multistability in grazing-sliding, namely $1 > T > 0$, $D > T^2$, $-C > 1$ and $T < \dfrac{-C-1}{C^2+C+1}$. The value of T is the product of the Floquet multipliers corresponding to the grazing orbit ignoring the interaction with the switching surface and D is the product of the multipliers. We found the non-sliding grazing orbit to be characterized by the Floquet multipliers $\lambda_1 = 0.025 + 0.5562i$ and $\lambda_2 = 0.025 - 0.5562i$, which implies that $T = 0.05$ and $D = 0.31$. The grazing orbit viewed as having a zero-length sliding segment is characterized by a non-trivial Floquet multiplier equal to $C = -3$. We note that in our dry-friction oscillator model, by means of a numerical continuation, we found a grazing-sliding bifurcation leading to multistability for the same values of the reduced map as in the constructed example of case I in Sec. 5. Similarly as in the constructed example model we observed that this scenario is sensitive to further parameter variations.

The nontrivial multiplier of the period-two orbit is equal to $\lambda_{P2} = -0.46$ and the non-trivial multiplier of the period-three orbit is equal to $\lambda_{P3} =$

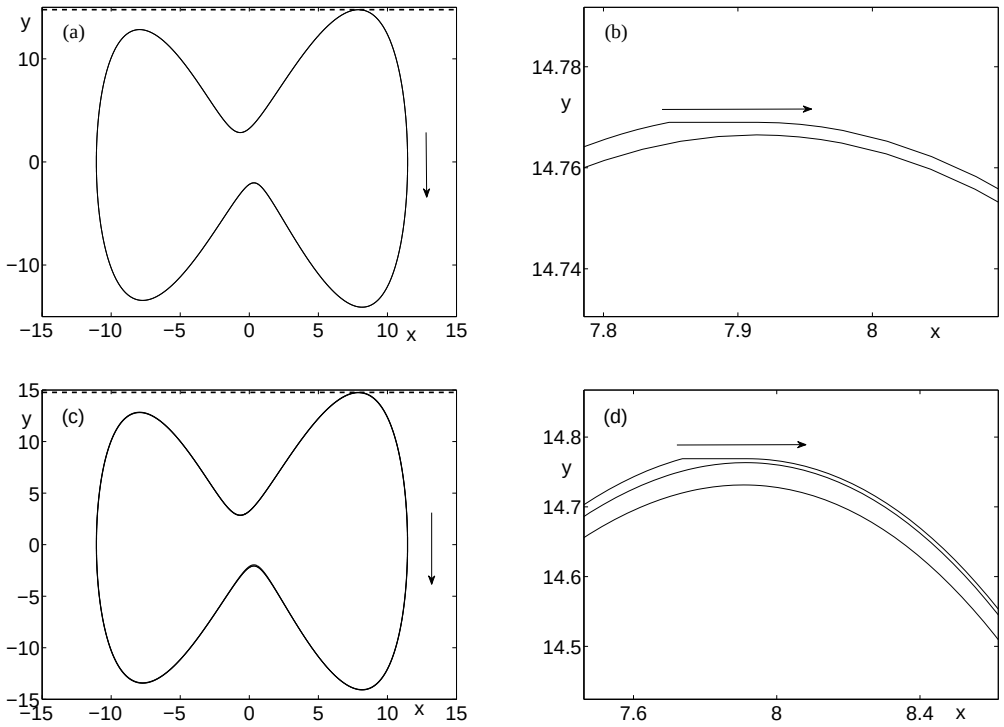

Figure 7: Phase plane $[x, y] = [x, \dot{x}]$. (a) Stable period-two orbit with a sliding segment born in the grazing-sliding bifurcation with initial values $[x, y, \tau] = [0.528502, -2.077219, 2.990137]$, and (b) zoom depicting the sliding segment of the orbit and a segment missing the switching surface. (c) Period-three stable attractor with sliding for initial values $[4.689348, 11.772725, 0.886640]$ and (d) zoom depicting a sliding segment and two segments of the orbit missing the switching surface. Initial values are given to six decimal places, though greater accuracy was used in the numerics.

0.9070, which values were found numerically by computing variational equations of the respective orbits. We could also use the normal form map given in [11] to compute the stability of the two limit cycles.

7. Conclusions

In this paper we have found, for the first time, an example of an explicit Filippov type flow where grazing-sliding bifurcation leads to the onset of multiple attractors. Three qualitatively different scenarios of multiple attractors in grazing-sliding bifurcations are shown. To find the parameter values for which these qualitatively different scenarios occur we use the analytical conditions reported in [11], where the classification of a one-dimensional normal form map for grazing-sliding bifurcations for three-dimensional Filippov type flows was conducted.

The theoretical predictions verified in this paper are based on the normal form for grazing sliding bifurcations [8]. This normal form is, by definition, local, in that it is derived by considering solutions near the periodic orbit at grazing in phase space and near the bifurcation value in parameter space. As with almost all such local theories, the domain on which the normal form is defined is not specified by the analysis, which holds for a 'sufficiently small' neighbourhood of the bifurcation. One of the consequences of our analysis is that it is possible to make some comments about how small 'small' really is in this example.

The attentive reader will have noted that the examples are shown for μ of the order of 10^{-3} to 10^{-6}. For larger, but still small, values of μ we observe dynamics which is different from that predicted, though in some cases it is consistent with the expectations of the normal form, but *not* for the parameter values we have so carefully chosen. In other words, had we simply matched behaviour in the flow with the general behaviour in the normal form we would have found no contradiction for some examples, but this would have been due to the fact that we were matching to parameters other than those that really apply. It is only at the smaller values of μ used in the reported simulations that the precise predictions of the normal form analysis are observed.

Then in Sec. 6 we investigated numerically a dry-friction oscillator model in view of finding any of the three cases of grazing-sliding bifurcations that would produce multistability. We found only one of the three cases; it is the first case of grazing-sliding bifurcations leading to multistability reported in

dry-friction oscillators. Similarly as in the constructed example the range of parameter values for which the stable orbits coexist past the bifurcation is small (Although larger than in the constructed example). Here, as noted earlier, the period three orbit gains an extra non-sliding segment which is not part of the grazing-sliding analysis within 0.003 of the bifurcation value of μ.

This poses two questions. First, why is 'small' so small (in smooth systems one can frequently get away with 10^{-2} or even larger)? It may of course be bad luck, and induction from just two examples is fool-hardy, but we could speculate that this is generally true for grazing bifurcations; the parameter $\sqrt{\mu}$ intervenes naturally here as the width of the sliding region, and small $\sqrt{\mu}$ implies very small μ.

Another feature that may have a bearing on this problem is that the corrections to the normal form are order $|x|^{\frac{3}{2}}$ rather than the standard x^2 terms for smooth systems – this is because the PDM is of the form

$$x_{n+1} = \mu + ax_n + b|x_n|^{\frac{3}{2}} + O(x^2). \tag{24}$$

Rescaling x by a factor of $|\mu|$ gives

$$X_{n+1} = \text{sign}(\mu) + aX_n + b\sqrt{|\mu|}|X_n|^{\frac{3}{2}} + O(\mu X^2) \tag{25}$$

and so the magnitude of μ is irrelevant for the truncated normal form, but the error term is $\sqrt{|\mu|}$, which is much larger than the $O(\mu)$ error in the smooth case.

The second question is about how normal forms are used. If the aim is simply to make the numerical results more reasonable theoretically, then it might not be necessary to obtain a precise correspondence between parameters in the normal form and parameters in the flow, but if the aim is to use the normal form as a predictive tool then the examples here underline the importance of ensuring that parameters really are close enough in the two cases. Whether our somewhat pessimistic view of the domain of strict applicability of the normal form analysis in nonsmooth sliding bifurcations is justified remains to be seen.

Our finding of the explicit Filippov flow with multiple attractors points to a number of research directions and open problems. Simpson has recently shown that the border collision normal form can have infinitely many coexisting stable periodic orbits [15]. It would be interesting to determine if this phenomenon can occur in grazing-sliding bifurcations of three-dimensional

type flows. It would also be interesting to use the idea for constructing explicit examples presented here to construct Filippov type flows where corner-collision bifurcations lead to the onset of multiple attractors. The question then arises if the possible pattern of emerging attractors is equivalent to the ones for grazing-sliding bifurcations. Finally, it might be possible to the use the knowledge on the existence on multiple attractors in grazing-sliding bifurcations as a control strategy. Suppose we have a Filippov system operating in some stable oscillatory state, can we use the knowledge on the existence of multiple attractors in discontinuity induced bifurcations to make our system evolve on some other attractor?

Acknowledgements PG and PK were partially funded by the CICADA project, EPSRC grant EP/E050441/1.

[1] S. Banerjee, C. Grebogi, Border collision bifurcations in two-dimensional piecewise smooth maps, Physical Review E 59 (1999) 4052–4061.

[2] S. Banerjee, P. Ranjan, C. Grebogi, Bifurcations in two-dimensional piecewise smooth maps – theory and applications in switching circuits, IEEE Transactions on Circuits and Systems – 1: Fundamental Theory and Applications 47 (2000) 633–643.

[3] S. Banerjee, G. Verghese, Nonlinear phenomena in power electronics: attractors, bifurcations, chaos, and nonlinear control, IEEE Press, New York, 2001.

[4] B. Brogliato, Impacts in mechanical systems — analysis and modelling, volume 551 of *Lecture Notes in Physics*, Springer-Verlag, 2000.

[5] H. Dankowicz, A. B. Nordmark, On the origin and bifurcations of stick-slip oscillations, Physica D 136 (1999) 280–302.

[6] H. de Jong, Modelling and simulations of genetic regulatory systems: A literature review, Journal of computational biology 9 (2002) 67–103.

[7] M. di Bernardo, P. Kowalczyk, A. Nordmark, Sliding bifurcations: A novel mechanism for the sudden onset of chaos in dry-friction oscillators, International Journal of Bifurcation and Chaos 13 (2003) 2935–2948.

[8] M. di Bernardo, C. Budd, A. Champneys, P. Kowalczyk, Piecewise-smooth Dynamical Systems — Theory and Applications, volume 163 of *Applied Mathematical Sciences*, Springer-Verlag, 2008.

[9] R. C. Dorf, R. H. Bishop, Modern control systems, Aeeizh, 2002.

[10] M. Dutta, H. E. Nusse, E. Ott, J. A. Yorke, G. Yuan, Multiple attractor bifurcations: A source of unpredictability in piecewise smooth systems, Physical Review Letters 83 (1999) 4281–4281.

[11] P. Glendinning, P. Kowalczyk, A. B. Nordmark, Attractors near grazing-sliding bifurcations, Nonlinearity 25 (2012) 1867–1885.

[12] A. B. Nordmark, P. Kowalczyk, A codimension-two scenario of sliding solutions in grazing-sliding bifurcations, Nonlinearity 19(1) (2006) 1–26.

[13] K. Popp, P. Stelter, Stick-slip vibrations and chaos, Philosophical Transactions: Physical Sciences and Engineering 332 (2000) 89–105.

[14] J. Sieber, Dynamics of delayed relay systems, Nonlinearity 19 (2006) 2489–2527.

[15] D.J.W. Simpson, Sequences of Periodic Solutions and Infinitely Many Coexisting Attractors in the Border-Collision Normal Form, International Journal of Bifurcation and Chaos 24 (2014) 1430018.

[16] R. Szalai, H.M. Osinga, Arnol′d Tongues Arising from a Grazing-Sliding Bifurcation, SIAM J. Appl. Dyn. Syst. 8 (2009) 1434–1461.